

Assessment of pancreatic colloid carcinoma using ^{18}F -FDG PET/CT compared with MRI and enhanced CT

LEI JIANG^{1-3*}, QIYING TANG^{2-4*}, CEDRIC M. PANJE^{5*}, HONGTING NIE⁶,
GUOCHAO ZHAO⁷ and HONGCHENG SHI¹⁻³

¹Department of Nuclear Medicine, Zhongshan Hospital, Fudan University; ²Nuclear Medicine Institute of Fudan University; ³Shanghai Institute of Medical Imaging; ⁴Department of Radiology, Zhongshan Hospital, Fudan University, Shanghai 200032, P.R. China; ⁵St Gallen Cantonal Hospital, St Gallen, CH-9000 Switzerland; ⁶Department of Pathology, Zhongshan Hospital, Fudan University; ⁷Department of General Surgery, Zhongshan Hospital, Fudan University, Shanghai 200032, P.R. China

Received December 4, 2017; Accepted May 22, 2018

DOI: 10.3892/ol.2018.8859

Abstract. Pancreatic colloid carcinoma (CC) is a rare sub-type of pancreatic adenocarcinoma which has an improved prognosis compared with pancreatic ductal carcinoma. Consequently, the early detection of CC by imaging may be of great significance in guiding patient management and therapeutic decisions. The present study aimed to analyze ^{18}F -FDG PET/CT findings of CC in comparison to MRI and CT. PET/CT findings in 5 patients with CC were retrospectively reviewed based on visual interpretation and semi-quantitative index of SUV_{max} and TNR. Four patients received dual-time-point PET/CT scans. Additionally, one patient underwent contrast-enhanced CT scan, one MRI, and three received both. A total of five lesions were detected in five patients. Visually, two cases presented with mild FDG uptake, two with moderate and one with high. The mean of SUV_{max} and TNR was 5.1 ± 2.2 and 2.8 ± 0.7 , respectively. Compared with CCs with low SUV_{max} , CCs with high SUV_{max} were more aggressive. No distant metastases were observed in five cases. Among four patients with dual-time-point PET/CT imaging, SUV_{max} increased in three cases and decreased in one case. The mean early and delayed SUV_{max} were 4.2 ± 1.1 and 4.7 ± 1.9 , respectively ($P > 0.05$). Radiological findings mainly included septated cystic components, internal sponge-like contrast-enhancement, calcification and 'salt-and-pepper sign' on MRI T2-weighted imaging. Thus, PET/CT provided additional information on metabolic tumor activity as well as locoregional and distant staging, which are important prognostic markers and may improve further patient management. However, PET/CT did not show any findings in addition to MRI and contrast-enhanced CT that were

unique to CC and allowed a clear differentiation from other pancreatic malignancies.

Introduction

Colloid carcinoma (CC), also known as mucinous non-cystic adenocarcinoma, is a distinctive type of invasive adenocarcinoma of the pancreas at the extreme well-differentiated end of the spectrum of pancreatic neoplasia (1). Pancreatic CC is a rare subtype that constitutes only 1-3% of invasive pancreatic adenocarcinomas (2). It is predominantly located in the head of the pancreas and almost always arises in association with intra-ductal papillary mucinous neoplasm (IPMN), especially the intestinal sub-type of IPMN. In addition, certain CCs involve the pancreatic tail and may originate from mucinous cystic neoplasms (MCN) (2,3). According to previous studies, CC is considered to exhibit a particularly indolent behavior with 5-year survival rates of 57-72% after resection, which is significantly better than for the more commonly found pancreatic ductal carcinoma (4,5).

At present, only small cases studies of CC of the pancreas on MRI and contrast-enhanced CT have been reported (6-12). However, due to the absence of the typical features on MRI and contrast-enhanced CT, it is always hard to distinguish CC from other pancreatic tumors, such as IPMN and MCN. To our knowledge, there have been no published reports about CC appearance on ^{18}F -FDG PET/CT imaging. In this study we present ^{18}F -FDG PET/CT findings in five cases with pancreatic CC as well as a correlation with their characteristics on MRI and contrast-enhanced CT.

Materials and methods

Patients. From January 2013 to August 2016, a total of five patients with histologically proven pancreatic CC, which underwent an ^{18}F -FDG PET/CT examination in our department, were identified and enrolled in this retrospective study. Additional imaging consisted of contrast-enhanced CT (n=1), MRI of the pancreas (n=1) or both modalities (n=3). The interval between FDG PET/CT and MRI or CT scans ranged from two to seven days. The institutional review board approved this

Correspondence to: Dr Hongcheng Shi, Department of Nuclear Medicine, Zhongshan Hospital, Fudan University, 180 Fenglin Road, Shanghai 200032, P.R. China
E-mail: shi.hongcheng@zs-hospital.sh.cn

*Contributed equally

Key words: pancreatic colloid carcinoma, ^{18}F -FDG, PET/CT, MRI, contrast-enhanced CT

study, and informed patient consent was obtained from all individual participants.

¹⁸F-FDG PET/CT scan. ¹⁸F-FDG PET/CT scan was performed on a Discovery VCT 64 system (GE Healthcare, Milwaukee, WI, USA) with 15.7 cm axial field view. Patients were required to fast for at least 6 h before imaging, and serum glucose levels were kept less than 7.4 mmol/l. Image was obtained approximately 60 min after intravenous administration of 3.7-5.6 MBq of FDG per kilogram of body weight. 6 or 7 bed positions from the base of skull to mid-thighs were imaged. PET images were acquired for 2.5 min per bed position. CT was performed on the same scanner without intravenous contrast administration. CT images were acquired with 140 kV, 200 mAs (adjusted by auto mA), and a gantry rotation speed of 0.8 sec. All CT scans were obtained using 3.75-mm-thick axial slices. Moreover, four out of five patients underwent an additional delayed (abdominal) PET/CT examination with an interval of ~90 min after the first scan.

Visual and semi-quantitative analysis of PET images. PET/CT results were retrospectively analyzed and interpreted by two experienced nuclear medicine physicians who were blinded to the patients' clinical data, previous radiological findings and pathology reports. Visual analysis grades of the pancreatic lesions were defined as follows by comparing the FDG uptake levels of the tumor to the surrounding normal tissue (13): grade 0 (no uptake), grade 1 (equivocal uptake), grade 2 (mildly increased and non-discrete uptake), grade 3 (mildly increased and discrete uptake), and grade 4 (definitely increased uptake). A result of grades 2-4 was considered to be positive, and a grade of 0 or 1 was considered to be negative. In case of discrepancy regarding the PET/CT findings, a consensus was reached after mutual discussion between the interpreting physicians. Areas of focally increased accumulation known to represent physiological ¹⁸F-FDG uptakes, such as brown fat, were excluded from the analysis.

For semi-quantitative analysis, maximum standard uptake value (SUV_{max}) and tumor-to-normal pancreatic tissue ratio (TNR) were analyzed. SUV_{max} was calculated as decay-corrected maximum activity concentration in the lesion divided by administered activity divided by body weight in kilograms. SUV_{max} of the normal pancreas was acquired as an average SUV_{max} of five regions of interest (ROIs) drawn on different segments of the normal pancreas. Each ROI was measured as a circle with a diameter of 1.5 cm. TNR was defined as SUV_{max} of the tumor divided by SUV_{max} of the normal pancreas tissue. In the case of a false-negative result on FDG PET, an ROI was placed over the area corresponding to the tumor displayed on CT and/or MRI.

MRI and contrast-enhanced CT examinations. MRI was performed using 1.5 Tesla MR unit (Magnetom Avanto, Siemens Medical Solutions, Germany). The conventional MR protocol used in this study included a transverse respiratory-triggered T2-weighted fat-suppressed turbo spin-echo sequence (TR/TE=2000/70 ms; section thickness: 5 mm; intersection gap: 2 mm; 320x224 matrix), and a transverse breath-hold three-dimensional T1-weighted, fat-suppressed spoiled gradient-recalled-echo sequence (TR/TE=209/4.8 ms; section thickness: 5 mm; intersection gap: 2 mm; 256x192 matrix). Multiphasic images consisting of arterial (35-45 sec), portal

Table I. Patient characteristics.

¹⁸ F-FDG PET/CT															
Case no.	Sex	Age (year)	CA 19-9 levels (ng/ml)	Tumor				SUV _{max}					CT	MRI	AJCC stage
				Location	Maximum diameter (cm)	Contour	Margin	Early	1.5 h delay	Normal pancreatic tissues	TNR	Retention index			
1	F	53	1540.0	Head	6.7	Iobulated	Relatively well-defined	3.0	3.2	1.3	2.3	6.7%	✓	✓	Ib
2	M	75	-	Body	3.5	Round	Indiscrete	3.5	2.9	1.3	2.7	-	-	✓	Ib
3	F	68	3108.0	Head and neck	2.7	Lobulated	Indiscrete	5.3	5.8	1.7	3.1	9.4%	✓	-	IIb
4	M	63	-	Head	5.0	Lobulated	Indiscrete	4.9	6.7	1.3	3.8	36.7%	✓	✓	IIa
5	M	72	-	Head	5.4	Lobulated	Well-defined	8.6	-	4.0	2.2	-	-	✓	IIa

TNR, tumor-to-normal pancreatic tissue ratio.

TNR, tumor-to-normal pancreatic tissue ratio.

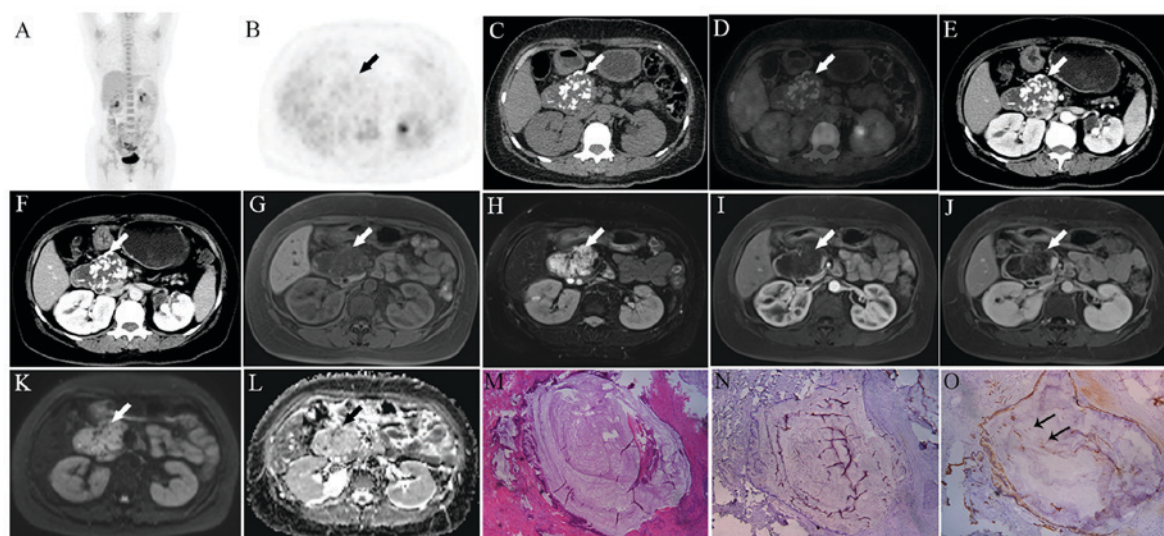


Figure 1. (Case 1). PET/CT showed the pancreatic lesion (arrow) with mild FDG uptake and without metastases [A, maximum intense projection (MIP); B, PET; C, CT; D, fused]. The SUV_{max} of the early and 1.5 h-delayed stages was 3.0 and 3.2, respectively, and the retention index was 6.7%. Contrast-enhanced CT showed a lesion of the pancreatic head (arrow) was mainly composed of cystic components and scattered calcification, and the capsule wall of the lesion was slightly enhanced (E, arterial stage; F, portal venous phase). Moreover, there was an apparent atrophy of the pancreatic body and tail and a dilation of pancreatic duct. MRI displayed the lesion (arrow) with low signal on T1WI (G) and high signal on T2WI (H). The septations were observed in the lesion, and were strongly enhanced (I, arterial stage; J, delayed phase). The lesion (arrow) showed also a high signal on DWI (K) and ADC (L) map. The lesion communicated with the main pancreatic. Mucinous cystic neoplasms (MCN) or intra-ductal papillary mucinous neoplasm (IPMN) was suspected based on contrast-enhanced CT and MRI. However, the pathological examination showed colloid carcinoma (CC) (M, H&E, magnification x100) with negative MUC1 (N, magnification x100) and positive MUC2 (O, magnification x100, arrows).

(70-80 sec), and delayed (120 sec) phases were acquired after the administration of 30 ml of contrast medium (gadopentetate dimeglumine, Magnevist; Bayer Healthcare, Berlin, Germany). Diffusion-weighted imaging (DWI) was acquired with two b values (0 and 500 sec/mm^2).

Triple-phase CT imaging was performed using Light Speed VCT (GE Healthcare, Milwaukee, WI, USA). A section thickness of 3 mm with a reconstruction interval of 3 mm, a field of view of 300-370 mm, a gantry rotation time of 0.5 sec, a tube current of 150-200 mA, and a peak voltage of 120 kVp were used. The detector collimation was 0.625 mm and the table speed was 46.8 mm per rotation, respectively. For contrast imaging, a fixed dose of 1.5 ml of iopromide per kilogram of body weight was administered at a rate of 2-3 ml/sec. The scanning time was delayed for the arterial and the portal venous phase for 35-45 and 70-80 sec following intravenous contrast administration, respectively.

MRI and contrast-enhanced CT analysis. The investigators analyzed MRI and/or CT features of the pancreatic tumors as follows: Lesion location; lesion size, measured as the longest diameter on the axial scan; contour and margin of the lesion; attenuation or signal intensity characteristics; enhancement features on dynamic images; presence and degree of ductal dilatation (main pancreatic duct ≥ 2 mm); calcification; and presence of other associated findings, such as adjacent organ invasion, lymph node involvement and distant metastases.

Pathological examination. All five patients underwent surgical resection of the intrapancreatic lesions for histopathologic confirmation within two weeks following FDG PET/CT imaging. Histopathology was reviewed by two experienced pathologists.

Statistical analysis. SPSS 18.0 software for Windows (SPSS Inc, Chicago) was used for statistical analysis. Data were expressed as mean \pm SD. The paired Student t test was used to compare the difference between SUV_{max} of early and delayed stages. The 95% confidence level was chosen to determine the significance between groups, with $P < 0.05$ indicating a significant difference.

Results

Patient characteristics. As shown in Table I, the five identified patients consisted of three males and two females with an average age of 66 ± 9 years (range 53-75 years). At the time of initial diagnosis, two patients presented with abdominal pain and distension, one patient presented with jaundice, fever and abdominal distention, and the remaining two lesions were incidentally found on imaging. CA 19-9 levels were normal in three patients and elevated in two patients, which were 1,540.0 and 3,108.0 U/ml (normal range < 37 U/ml), respectively.

All five patients underwent surgical resection of the tumors, which was performed as pancreaticoduodenectomy in four patients, and distal pancreatectomy in one patient. Moreover, one patient with CC in the head and neck of the pancreas underwent an additional dissection of the hepatoduodenal ligament lymph nodes because of invasion of Glisson's sheath. Three lesions were located in the pancreatic head, one in the head and neck, and one in the body. The mean maximum diameter of the tumors on axial imaging was 4.7 ± 1.6 cm (range 2.7-6.7 cm).

^{18}F -FDG PET/CT findings. On visual analysis, the FDG uptake of tumor slightly higher than that of the surrounding pancreatic parenchyma was observed in case 1 (Fig. 1) and case 2

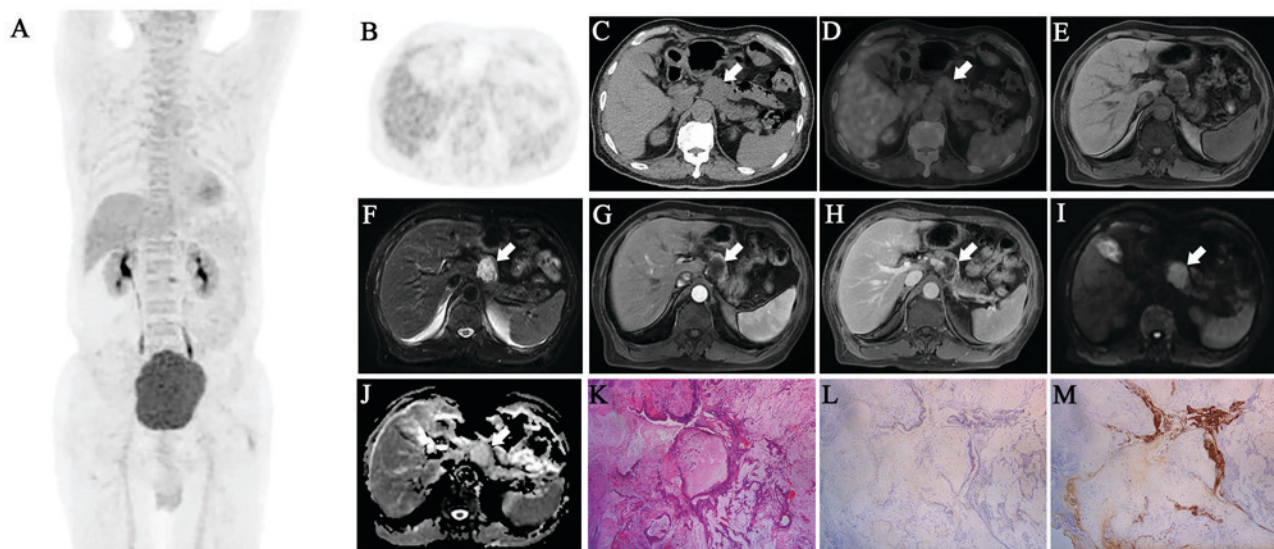


Figure 2. (Case 2). PET/CT showed a lesion (arrow) with mild FDG uptake with a SUV_{max} of 3.5, and no distant metastases (A, MIP; B, PET; C, CT; D, fused). On the 1.5 h-delayed stage, SUV_{max} decreased to 2.9. MRI showed the pancreatic lesion (arrow) with low signal on T1WI (E), and high signal on T2WI (F). The lesion (arrow) was mildly enhanced on the enhanced arterial phase (G), and was further filled with contrast agent in the delayed phase (H) with additional peripheral enhancement. The lesion (arrow) showed also a high signal on DWI (I) and ADC (J) map. Therefore, a solid pseudo papillary tumor (SPT) was suspected based on imaging findings, but pathology confirmed a colloid carcinoma (CC) (K, H&E, magnification x100) with negative MUC1 (L, magnification x100) and positive MUC2 (M, magnification x100, arrows).

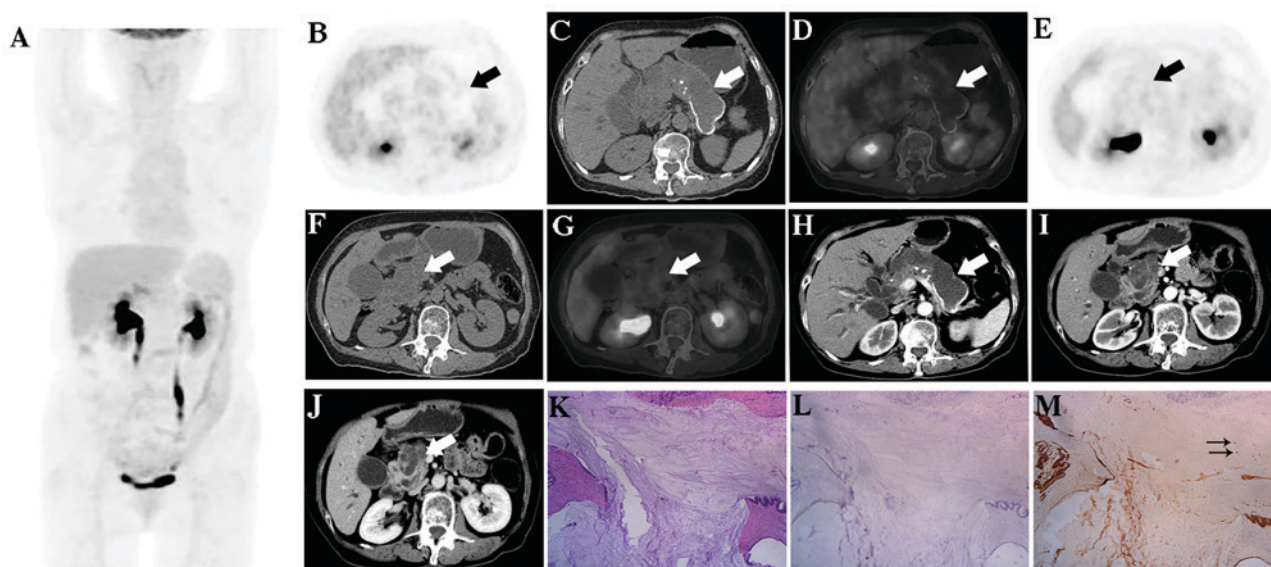


Figure 3. (Case 3). PET/CT [A, MIP; B and E, PET; C and F, CT; D and G, fused) displayed the significantly enlarged pancreatic duct (B-D) arrow] and the lesion of pancreatic head and neck (E-G), arrow) with moderate uptake of FDG, and SUV_{max} of the early and 1.5 h-delayed lesion was 5.3 and 5.8, respectively, and the retention index was 9.4%. No local invasion and distant metastases were observed on PET/CT imaging. Contrast-enhanced CT displayed the enlarged pancreatic duct (H, arrow) and a multi-cystic lesion (I and J, arrow) communicating with the pancreatic duct. The capsule wall and septations of the mass were mildly enhanced. Moreover, dilated intra-hepatic and extra-hepatic bile ducts and an enlarged gallbladder were observed. Thus, intra-ductal papillary mucinous neoplasm (IPMN) was firstly considered by the radiologists. The pathology confirmed colloid carcinoma (CC) (K, H&E, magnification x100) with negative MUC1 (L, magnification x100) and positive MUC2 (M, magnification x100, arrows) and additional involvement of three metastatic lymph nodes in the Glisson's sheath.

(Fig. 2), moderately higher in case 3 (Fig. 3) and 4 (Fig. 4), and considerably higher in case 5 (Fig. 5). Although the SUV_{max} of the CC lesion was 8.6 in case 5, the remaining pancreatic parenchyma SUV_{max} was 4.0, which corresponded to inflammation in histopathology. For five lesions, the mean of early SUV_{max} was 5.1 ± 2.2 , with a variability of SUV_{max} ranging from 3.0 to 8.6, and the average of TNR was 2.8 ± 0.7 , with the range from 2.2 to 3.8.

Four patients underwent both early and 1.5 h-delayed PET/CT examinations. The mean SUV_{max} of the early and delayed stages were 4.2 ± 1.1 (range, 3.0-5.3), and 4.7 ± 1.9 (range, 2.9-6.7), respectively, and there was no significant difference between SUV_{max} of the early and delayed stages ($P > 0.05$). The SUV_{max} increased in three cases, and decreased in one case. The retention index in the three cases with increasing SUV_{max} was 6.7, 9.4 and 36.7%, respectively, and the average was $17.6 \pm 16.6\%$.

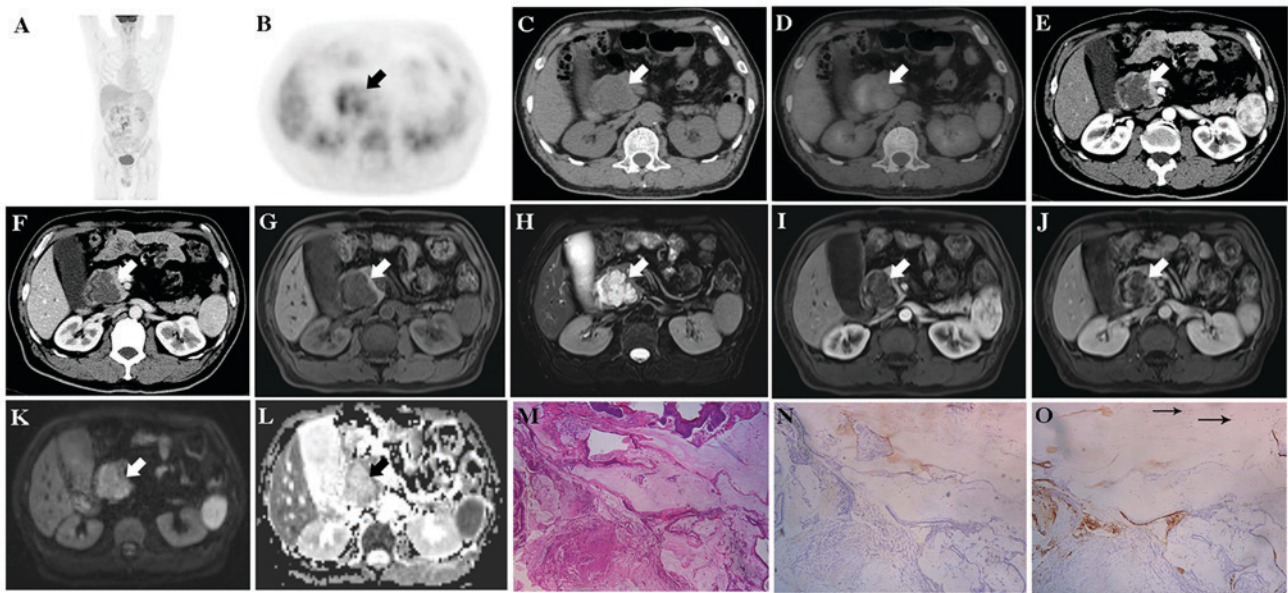


Figure 4. (Case 4). PET/CT (A, MIP; B, PET; C, CT; D, fused) displayed a strong uptake of FDG by the pancreatic lesion (arrow), and the SUV_{max} of early and 1.5 h-delayed stages were 4.9 and 6.7, respectively, and the retention index was 36.7%. CT showed a slightly enhancing lesion (arrow) on the arterial phase (E) that was further filled with the contrast agent on the portal vein phases (F). MRI displayed a lesion (arrow) with low signal on T1WI (G) and high signal on T2WI (H), and a similar enhancement pattern to CT (I, arterial stage; J, delayed phase). The lesion (arrow) showed also a high signal on DWI (K) and ADC (L) map. Moreover, the boundary between the lesion and the duodenal descending segment was detectable on imaging. Intra-ductal papillary mucinous neoplasm (IPMN) was considered by the radiologists, but pathology diagnosed a colloid carcinoma (CC) (M, H&E, magnification x100) which was negative for MUC1 (N, magnification x100) and positive for MUC2 (O, magnification x100, arrows).

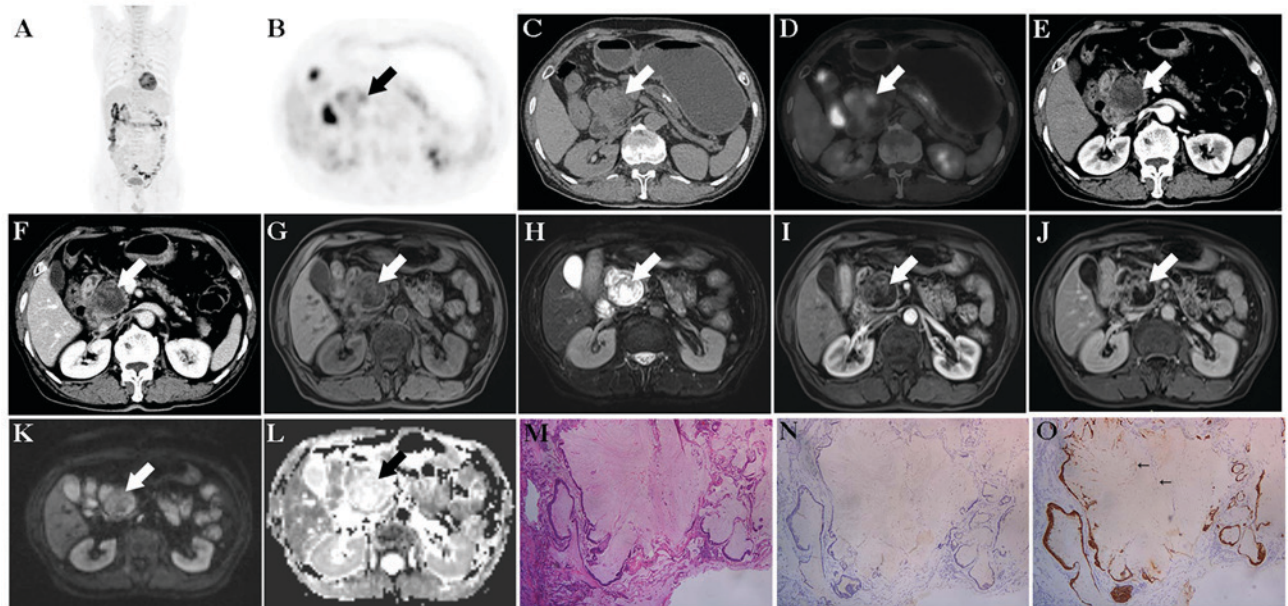


Figure 5. (Case 5). PET/CT (A, MIP; B, PET; C, CT; D, fused) displayed that the lesion of the pancreatic head (arrow) had a strong FDG uptake and the SUV_{max} was 8.6. The pancreatic body and tail showed apparent atrophy and calcification as well as diffuse FDG accumulation with a SUV_{max} of 4.0. FDG accumulated also in the adjacent duodenum and the SUV_{max} was 12.9. Moreover, a non-specific inflammation in mediastinal and bilateral hilar lymph nodes was observed (A). CT showed a solid-cystic mass (arrow) in the pancreatic head, and the solid parts were progressively enhancing (E, arterial stage; F, portal venous phase). MRI displayed the lesion (arrow) with heterogeneous signal, with iso-intense or low signal on T1WI (G), and high signal on T2WI (H) and additional dilation of pancreatic duct. The lesion (arrow) was heterogeneously enhancing (I, arterial stage; J, delayed phase) and showed a high signal on DWI (K) and on the ADC (L) map. Therefore, mucinous cystic neoplasms (MCN) was initially considered, but the pathological exam confirmed the presence of CC in the pancreatic head (M, H&E, magnification x100) with negative MUC1 (N, magnification x100) and positive MUC2 (O, magnification x100, arrows) as well as the pancreatitis of the body and tail.

MRI and contrast-enhanced CT findings. Four patients received MRI scans (cases 1, 2, 4 and 5). CCs showed heterogeneously hypo-intense signals on T1-weighted images

and heterogeneously hyper-intense signals on T2-weighted images which were brighter than the spleen. Additionally, there was spot-like and streak-like hypo-attenuation

observed within the tumors on T2-weighted images. On gadolinium-enhanced MR images, the solid portions or septations of the lesions were progressively enhancing, which could be described as sponge-like enhancement pattern. The tumors of patients 1 and 2 showed additional peripheral enhancement. Pancreatic upstream ductal dilation was found in three cases, including cases 1, 3 and 5, and two lesions were communicating with the pancreatic duct (cases 1 and 3).

Four patients underwent additional abdominal contrast-enhanced CT examination (cases 1, 3, 4 and 5). CCs showed predominantly a cystic component with septations on CT images. The solid portions and septations of tumor showed a slight hyper-attenuation or iso-attenuation on pre-contrast CT, weak enhancement during the arterial phase on contrast-enhanced CT and increasing enhancement in the portal venous phase. All four lesions showed internal sponge-like enhancement pattern, which was less visible on CT than on MRI. Moreover, calcifications in different patterns were observed in three cases with CCs (cases 1, 3 and 5): One case with coarse calcification in the lesion (case 1), one case with punctate and eggshell calcification in the enlarged pancreatic duct (case 3) and one case with coarse calcification in the non-lesion part of the pancreas with pancreatitis (case 5).

Pathological findings. All five cases were histologically confirmed CCs which were negative for MUC1 expression and positive for MUC2. Case 1 and case 2 did not show any lymph node metastasis or invasion of adjacent organs. The Glisson's sheath was invaded by CC in case 3 where three positive lymph nodes were found. The remaining two cases of CC (cases 4 and 5) were located in the pancreatic head and invaded the duodenum. Moreover, based on the American Joint Committee on Cancer (AJCC) TNM staging system (7th edition) (14), two cases were staged as Ib, one case as stage IIa and two cases as stage IIb (Table I).

Discussion

CC of the pancreas was first described in a case report by Muir in 1952 (15). Owing to the ambiguity in the classification and lack of awareness of this entity, many CCs of the pancreas have been categorized as ordinary ductal adenocarcinoma, or misdiagnosed as IPMN, MCN or signet-ring cell adenocarcinoma (2). In a pathological study of 17 patients diagnosed with pancreatic CC in 2001, Adsay *et al* (4) considered it as a rare mucous-producing tumor that should be distinguished from other pancreatic neoplasms. According to the Armed Forces Institute of Pathology (AFIP) definition in 2007, the colloid component of CC should comprise at least 80% of the neoplasm (1).

Compared with pancreatic ductal adenocarcinoma, CC usually shows an indolent clinical behavior with a slower growing pattern and better prognosis (16). The different clinical behavior may be in part related to two characteristic features of this tumor: a) altered tumor-cell polarity found in microscopic examination where the stromal cell surface demonstrates secretory properties instead of a ductal cell surface, and b) the type of mucin secreted by the tumor cells (17). Both MUC1 and MUC2 seem to have important

roles in pancreatic neoplasia. MUC1 appears to be a marker of an aggressive phenotype and may facilitate vascular spread of tumor cells. MUC2 is commonly expressed in tumors with an indolent course, such as some IPMNs and specifically in CCs involving different organs (16,17). It has been postulated that the secretion of MUC2 into the stroma provokes the formation of a gelatinous layer of mucin around the tumor cells that would limit their metastatic spread (17,18).

It has been reported that CCs yield a 5-year survival rate ranging from 57-72% in resectable cases (4,5). Therefore, it is paramount to identify patients eligible for surgical treatment using radiological staging. CCs on CT usually appear as masses with round or lobular margins and usually have clear boundaries. The exception is that some tumors may have ill-defined boundaries towards the duodenum that indicates invasion to the duodenum (10), such as cases 4 and 5 in this study. CCs predominantly present with cystic components with septations, which show hyper-attenuation or iso-attenuation on pre-contrast CT, weak enhancement during the arterial phase on contrast-enhanced CT, and increasing enhancement in the portal venous phase. In our series, four of five cases have the similar appearance. Additionally, calcification was also observed in CCs, and the most likely explanation for the calcification in CCs is the presence of thick mucin, which has the tendency to build up calcium salt deposits (19,20).

There is limited information on the morphological appearance of pancreatic CC on MR imaging. Yoon *et al* (12) described the appearance of CC on MRI as a mass with lobulated contours and indistinct margins that exhibited a hyper-intense salt-and-pepper-like appearance on T2-weighted imaging with peripheral and internal sponge-like or mesh-like progressive delayed contrast enhancement. These findings were confirmed by our study. Moreover, Yoon *et al* (12) suggested that the distinction of CC from IPMN could be made with greater confidence based on the absence of pancreatic ductal communication or downstream ductal dilation in MRCP. However, in our study, three cases of CCs presented with upstream pancreatic ductal dilation and two lesions even communicated with the pancreatic duct. CCs usually arise from IPMN, thus the communication between the tumors and the pancreatic duct is possible and reasonable (2,3). In addition, none of the CCs in our study showed intra-ductal papillary components or bulging of the papilla of Vater into the duodenal lumen, which are common findings in IPMN (21). We found that CCs displayed hyper-intense on both DWI and ADC map, which reflects the low cellularity and fluid-rich environment of CC and results in greater freedom of motion of water molecules (22).

Combined morphological and metabolic imaging, FDG PET/CT has proven to be a valuable diagnostic tool in pancreatic cancer which may provide, apart from improved staging for lymph nodes and distal metastasis, additional prognostic information depending on the SUV_{max} of the primary tumor (13,23,24). To our knowledge, this study is the first and largest series of CCs imaged by FDG PET/CT. All CCs except one case showed a mild to moderate FDG uptake judged by visual interpretation. However, in the single case with elevated FDG uptake, histopathological evaluation of the surgical specimen revealed pancreatitis, which may most likely be the reason of the increased FDG uptake. While the

limited number of cases did not allow any further statistical analysis, AJCC stage I tumors showed SUV_{max} of 3.0 and 3.5 respectively, while more advanced tumors which showed local invasion into the duodenum or lymph node metastases on histopathology presented with higher SUV_{max} ranging from 4.9 to 8.6. These findings are in congruence with a recent meta-analysis that showed a prognostic value for SUV_{max} for pancreatic tumors (24). Finally, no distant metastases were observed on ^{18}F -FDG PET/CT imaging in all five cases, which reflects that the less aggressive growth pattern of CC with better prognosis compared to ductal adenocarcinoma. While FDG-PET/CT provided additional information regarding locoregional and distal metastases as well as on the FDG uptake of the primary, dual-time-point PET/CT scan showed only relatively small changes in SUV_{max} between the early and delayed stages. Therefore, the value of dual-time-point imaging of PET/CT in the assessment of CC remains to be elucidated.

In conclusion, CC of the pancreas do not have typical features on CT and MRI and are therefore hard to distinguish from other pancreatic tumors such as IPMN and MCN. ^{18}F -FDG PET/CT did not show tumor characteristics which were unique to CC, but provided important information on potential locoregional and distant metastases as well as on metabolic tumor activity which may improve further patient management. The presence of CC should be considered when a pancreatic tumor presents with a predominantly cystic pattern with septations and sponge-like enhancement, calcifications, upstream pancreatic ductal dilation, the presence of the 'salt-and-pepper sign' on T2-weighted MRI, mild to moderate FDG uptake and the absence of distant metastases.

Acknowledgements

Not applicable.

Funding

This study was supported in part by the National Science Foundation for Scholars of China (grant no. 81571703) and funding sponsored by Shanghai Pujiang Program (grant no. 2015PJD006).

Availability of data and materials

All data generated or analyzed during this study are included in this published article.

Authors' contributions

HS and LJ conceived and designed the study. LJ, QT, HN, CMP and GZ collected and analyzed the imaging and pathology data. LJ, QT and CMP wrote the paper. CMP also edited the paper.

Ethics approval and consent to participate

This retrospective study was approved by the ethics committee of Zhongshan hospital. Informed consent to participate was obtained from the patients.

Consent for publication

The patients of our study provided written informed consent for the publication of any associated data and accompanying images.

Competing interests

The authors declare that they have no competing interests.

References

1. Hruban R, Pitman M and Klimstra D: AFIP Atlas of Tumor Pathology. Tumors of the Pancreas. 4th Series, Fascicle 6. Washington: American Registry of Pathology, American Registry of Pathology and Armed Forces Institute of Pathology, Washington, DC, 2007.
2. Liszka L, Zielinska-Pajak E, Pajak J and Gołka D: Colloid carcinoma of the pancreas: Review of selected pathological and clinical aspects. *Pathology* 40: 655-663, 2008.
3. Seidel G, Zahurak M, Iacobuzio-Donahue C, Sohn TA, Adsay NV, Yeo CJ, Lillmoie KD, Cameron JL, Hruban RH and Wilentz RE: Almost all infiltrating colloid carcinomas of the pancreas and periampullary region arise from in situ papillary neoplasms: A study of 39 cases. *Am J Surg Pathol* 26: 56-63, 2002.
4. Adsay NV, Pierson C, Sarkar F, Abrams J, Weaver D, Conlon KC, Brennan MF and Klimstra DS: Colloid (mucinous noncystic) carcinoma of the pancreas. *Am J Surg Pathol* 25: 26-42, 2001.
5. D'Angelica M, Brennan MF, Suriawinata AA, Klimstra D and Conlon KC: Intraductal papillary mucinous neoplasms of the pancreas: An analysis of clinicopathologic features and outcome. *Ann Surg* 239: 400-408, 2004.
6. Escalon JG, Gerst S, Porembka M, Allen PJ and Do RK: Imaging comparison of tubular and colloid pancreatic adenocarcinoma arising from intraductal papillary mucinous neoplasm on multi-detector CT. *Clin Imaging* 40: 1195-1199, 2016.
7. Gao Y, Zhu YY and Yuan Z: Colloid (mucinous non-cystic) carcinoma of the pancreas: A case report. *Oncol Lett* 10: 3195-3198, 2015.
8. Jung JY, Song MH, Park YS, Jo YJ, Kim SH, Jun DW, Kim DH and Lee WM: A case of mucinous noncystic carcinoma of the pancreas. *Korean J Gastroenterol* 51: 204-208, 2008 (In Korean).
9. Plerhoples TA, Ahdoot M, DiMaio MA, Pai RK, Park WG and Poultides GA: Colloid carcinoma of the pancreas. *Dig Dis Sci* 56: 1295-1298, 2011.
10. Ren FY, Shao CW, Zuo CJ and Lu JP: CT features of colloid carcinomas of the pancreas. *Chin Med J (Engl)* 123: 1329-1332, 2010.
11. Rubio-Perez I, Martin-Perez E, Sanchez-Urdazpal L, Corbaton P and Larrañaga E: Colloid carcinoma of the pancreas: A distinct pancreatic neoplasm with good prognosis. Report of a case. *JOP* 13: 219-221, 2012.
12. Yoon MA, Lee JM, Kim SH, Lee JY, Han JK, Choi BI, Choi JY, Park SH and Lee MW: MRI features of pancreatic colloid carcinoma. *AJR Am J Roentgenol* 193: W308-W313, 2009.
13. Jiang L, Tan H, Panje CM, Yu H, Xiu Y and Shi H: Role of ^{18}F -FDG PET/CT imaging in intrahepatic cholangiocarcinoma. *Clin Nucl Med* 41: 1-7, 2016.
14. Edge SB, Byrd DR, Compton CC, Fritz AG, Greene FL and Trotti A (eds): AJCC Cancer Staging Manual. 7th edition, Springer, New York, NY, 2010.
15. Muir EG: Colloid carcinoma of the pancreas. *Br J Surg* 40: 177, 1952.
16. Nakata K, Ohuchida K, Aishima S, Sadakari Y, Kayashima T, Miyasaka Y, Nagai E, Mizumoto K, Tanaka M, Tsuneyoshi M and Oda Y: Invasive carcinoma derived from intestinal-type intraductal papillary mucinous neoplasm is associated with minimal invasion, colloid carcinoma, and less invasive behavior, leading to a better prognosis. *Pancreas* 40: 581-587, 2011.
17. Adsay NV, Merati K, Nassar H, Shia J, Sarkar F, Pierson CR, Cheng JD, Visscher DW, Hruban RH and Klimstra DS: Pathogenesis of colloid (pure mucinous) carcinoma of exocrine organs: Coupling of gel-forming mucin (MUC2) production with altered cell polarity and abnormal cell-stroma interaction may be the key factor in the morphogenesis and indolent behavior of colloid carcinoma in the breast and pancreas. *Am J Surg Pathol* 27: 571-578, 2003.

18. Levi E, Klimstra DS, Andea A, Basturk O and Adsay NV: MUC1 and MUC2 in pancreatic neoplasia. *J Clin Pathol* 57: 456-462, 2004.
19. Kalaitzakis E, Braden B, Trivedi P, Sharifi Y and Chapman R: Intraductal papillary mucinous neoplasm in chronic calcifying pancreatitis: Egg or hen? *World J Gastroenterol* 15: 1273-1275, 2009.
20. Zapiach M, Yadav D, Smyrk TC, Fletcher JG, Pearson RK, Clain JE, Farnell MB and Chari ST: Calcifying obstructive pancreatitis: a study of intraductal papillary mucinous neoplasm associated with pancreatic calcification. *Clin Gastroenterol Hepatol* 2: 57-63, 2004.
21. Song SJ, Lee JM, Kim YJ, Kim SH, Lee JY, Han JK and Choi BI: Differentiation of intraductal papillary mucinous neoplasms from other pancreatic cystic masses: Comparison of multirow-detector CT and MR imaging using ROC analysis. *J Magn Reson Imaging* 26: 86-93, 2007.
22. Wang Y, Miller FH, Chen ZE, Merrick L, Morteale KJ, Hoff FL, Hammond NA, Yaghmai V and Nikolaidis P: Diffusion-weighted MR imaging of solid and cystic lesions of the pancreas. *Radiographics* 31: E47-E64, 2011.
23. Jha P and Bijan B: PET/CT for pancreatic malignancy: Potential and pitfalls. *J Nucl Med Technol* 43: 92-97, 2015.
24. Wang Z, Chen JQ, Liu JL, Qin XG and Huang Y: FDG-PET in diagnosis, staging and prognosis of pancreatic carcinoma: A meta-analysis. *World J Gastroenterol* 19: 4808-4817, 2013.



This work is licensed under a Creative Commons Attribution-NonCommercial-NoDerivatives 4.0 International (CC BY-NC-ND 4.0) License.